TESTS AND PERFORMANCE ANALYSIS OF THE DMC AT THE CARTOGRAPHIC INSTITUTE OF CATALONIA (ICC)

W. Kornus, R. Alamús, J. Talaya

Institut Cartogràfic de Catalunya, Parc de Montjuïc, 08038 Barcelona, Spain

KEY WORDS: Digital camera, accuracy, automatic DEM, self-calibration

ABSTRACT:

The ISPRS congress in Amsterdam in 2000 raised great expectations in matrix-CCD based digital cameras for aerial photogrammetry and mapping applications. During the last two years the number of large format digital cameras in the market has increased significantly. In 2004 the Cartographic Institute of Catalonia (ICC) purchased a Digital Mapping Camera (DMC) of the ZEISS/INTERGRAPH (Z/I) company and started a comprehensive evaluation and validation process with the final goal to complete and optimize a fully digital photogrammetric workflow and also to analyze and exploit the full DMC accuracy potential. The paper focuses mainly on the role of self-calibration parameters and the assessment of automatic digital elevation model (DEM) accuracy as quality test for the DMC. The results of a series of block triangulations are discussed in comparison to the outcome of corresponding RC30 analog block triangulations. Furthermore, automatically derived DEM both from DMC and RC30 are compared to a Lidar reference DTM. It is concluded, that an appropriate self-calibration model is mandatory to fully exhaust the DMC accuracy potential, which has been discussed in early literature.

1. INTRODUCTION

In 2004 the Institut Cartogràfic de Catalunya (ICC) decided to make a commitment to a totally digital mapping workflow. Once the selection phase for a digital camera had been completed, a ZEISS/INTERGRAPH (Z/I) Digital Mapping Camera (DMC) was delivered to the ICC. Following this, the ICC needed to validate, evaluate and find the most suitable strategy to get the better performance of the DMC. Several blocks have been aerotriangulated and studied in detail in order to assess the potential accuracy of the new camera and to investigate the changes on the current photogrammetric models that the new technology may require. This paper focuses mainly on the role of self-calibration parameters and the assessment of automatic DEM quality as quality test for the DMC.

2. DATA SETS

2.1 Block 'Amposta'

On 16th December 2004 image data of the Amposta block was taken. The block consists of 139 images distributed in 5 parallel and 2 transversal strips, taken at a flight altitude of 800 m above ground level, which corresponds to a ground sampling distance (GSD) of 8 cm. The block contains 7 full ground control points (GCP), 6 check points and 139 GPS/INS aerial control points.

The performance of the DMC was assessed and compared to the aerotriangulation results of the same block flown with an analog camera in 2000. The analog block consists of 69 photographs distributed in 5 parallel strips and 2 transversal strips (exactly the same configuration as the aforementioned DMC block). The block contains 8 full GCP and 1 check point. The 7 full GCP used in the DMC block are a subset of the 8 GCP in the analog block. The 8th point could not be measured in the DMC images. The analog check point is one of the 6 check points used in the DMC block.

2.2 Block 'Rubí'

The data relating to Rubí was acquired on 8th March 2005. The block consists of 426 images distributed in 13 parallel and 3 transversal strips, taken at a flight altitude of 1000 m above ground level, which corresponds to a GSD of 10 cm. 19 GCP and 426 GPS/INS aerial control points were used to aerotriangulate the block. Moreover, 20 well distributed check points were measured in the images, which belong to the fourth order Geodetic Network of Rubí and have an accuracy of 2 cm in planimetry and 4 cm in altimetry.

2.3 Block '415'

The 415 block covers a rectangular area of 90 km x 20 km, which is the area covered by three 1:50 000 sheets. The block consists of 312 images distributed in 4 parallel and 2 transversal strips, taken at an average altitude of 4 700 m above ground level, which corresponds to a GSD of 0.47 m. The block contains 33 full GCP, 18 check points and 312 GPS aerial control points. Furthermore, some areas of the block are covered by a Lidar DTM/DEM. In these areas a study of DMC automatic DEM accuracy has been conducted (see section 3.3).

2.4 Block '419'

The 419 block covers a rectangular area of 30 km x 20 km, which is the area covered by a single 1:50 000 sheet. The block consists of 98 images, distributed in 4 parallel strips, taken at an average altitude of 4700 m above ground level, which corresponds to a GSD of 0.47 m. The block contains 26 full GCP and 98 GPS/INS aerial control points.

3. ANALYSIS OF RESULTS

3.1 Aerotriangulation results

The results of DMC aerotriangulation were assessed both in image and in object space in comparison to correspondent aerotriangulations of conventional analog images.

3.1.1 Pointing accuracy

To assess the pointing accuracy the block Amposta was aerotriangulated three times:

1. using manual photogrammetric observations from analog RC30 images
2. using manual photogrammetric observations from DMC images
3. using automatic photogrammetric observations from DMC images (Match-AT)

In the first case 188 photogrammetric observations were manually measured in the analog RC30 images corresponding to 217 tie points, 8 full GCP and 1 check point. The images were scanned at 15 µm pixel size. 69 GPS aerial control points, one set of linear drift parameters per strip and one set of 12 self-calibration parameters were used in the block adjustment.

In the second case 757 photogrammetric observations were manually measured in the DMC images, corresponding to 431 tie points, 7 full GCP and 6 check control points. 139 full GPS/IMU aerial control points, one set of linear drift parameters per strip and no self-calibration parameters were used in the block adjustment. The photogrammetric model is described in Baron et al. (2003).

In the third case 17 068 photogrammetric observations of 3 068 tie points were automatically derived from the same DMC images by Inpho's Match-AT software using the same control and check point configuration. All 3D data refer to projective UTM coordinates. Since Match-AT works exclusively with Cartesian coordinates, the bundle block adjustments were carried out—as in all the other cases of this study—with the in-house ACX-GeoTex software (Colomina et al., 1992); i.e. Match-AT was exclusively used for the automatic production of photogrammetric observations.

	Analog manual		DMC manual		DMC automatic	
	µm	pix.	µm	pix.	µm	pix.
x	4.83	0.32	2.85	0.24	1.23	0.10
y	4.27	0.29	2.35	0.20	1.12	0.09

Table 1: RMS of photogrammetric residuals after block adjustments using manually measured points in analog images scanned at 15 µm pixel size (Analog manual), manually measured points in DMC images (DMC manual) and automatically matched points in DMC images (DMC automatic).

Table 1 shows the root mean squared values (RMS) of all photogrammetric residuals after bundle block adjustments, which is a reliable measure for the pointing accuracy. The accuracy improves by a factor of 1.3 comparing manual point identification in DMC images to analog images, and even by a factor of 3 if comparing digital image matching in DMC images to manual point identification in analog images.

3.1.2 Pointing accuracy

The 3D point accuracy is assessed using independent check points. Table 2 shows the statistics on the differences between the check point coordinates and the aerotriangulation results of the blocks Amposta, Rubí and 415. It must be noted, that the blocks Rubí and 415 were adjusted with 4 sets of self-calibration parameters, while the Amposta block was calculated without self-calibration (see section 3.2).

Block	Points	GSD [cm]		Mean [m]	RMS [m]	σ [m]	$\sigma_{predicted}$ [m]
Amposta	6	8.0	X	-0.05	0.06	0.04	0.03
			Y	0.01	0.02	0.02	0.03
			H	-0.02	0.04	0.04	0.04
Rubí	20	10.0	X	-0.00	0.04	0.04	0.04
			Y	0.00	0.03	0.03	0.04
			H	-0.02	0.06	0.06	0.05
415	18	47.0	X	-0.09	0.25	0.24	0.20
			Y	-0.05	0.26	0.26	0.20
			H	0.17	0.30	0.26	0.24

Table 2: Statistics on the check point accuracies (σ). $\sigma_{predicted}$ is the predicted accuracy according to Dörstel (2003).

In Dörstel (2003) the predicted accuracies of a DMC aerotriangulation are outlined to be 5 µm times the image scale in planimetry and 0.05‰ of the flying altitude in height, which corresponds to 3 cm in planimetry and 4 cm in height for the Amposta and Rubí blocks. The respective results in table 2 are fully consistent in planimetry and a little worse in height. More results are described in Alamús et al. (2005), which demonstrate that analog cameras and the DMC achieve comparable 3D point accuracies in aerotriangulation and also in stereoplotting.

3.2 The role of self-calibration parameters

This section analyzes a possible improvement of the DMC accuracy potential by the application of self-calibration parameters. The Rubí block was aerotriangulated three times using the same image, control (ground and aerial) and check observations and the same image tie points, generated by Match-AT: Firstly, without self-calibration, secondly, with one set of 12 self-calibration parameters (Ebner, 1976) and finally, with four sets of 12 self-calibration parameters. These four sets are related to the four quarters of the DMC image, which are acquired by four different high resolution DMC camera heads. This approach pays tribute to the special DMC design and enables self-calibration of each single camera head. For more information about the DMC geometry see Hinz (1999) and Dörstel et al. (2003).

		No self-calibration	1 parameter set	4 parameter sets
Residuals [pixel]	x	0.15	0.14	0.14
	y	0.11	0.11	0.11
Checkpoint-accuracy [m]	X	0.03	0.04	0.04
	Y	0.05	0.04	0.03
	H	0.15	0.15	0.06

Table 3: Impact of self-calibration parameters on the standard deviations of the image residuals and the ground coordinates at the 20 check points of the Rubí block.

Table 3 and figure 1 demonstrate impressively the impact of 4 sets of self-calibration parameters on the photogrammetric object reconstruction. A single set of 12 parameters does not significantly improve the statistics of neither the photogrammetric residuals nor the final accuracy at the check points although 7 of the 12 parameters are estimated significantly with values up to 12 times larger than their standard deviations. With 4 sets of 12 self-calibration parameters the height standard deviations at the check points decrease from 15 cm to 6 cm.

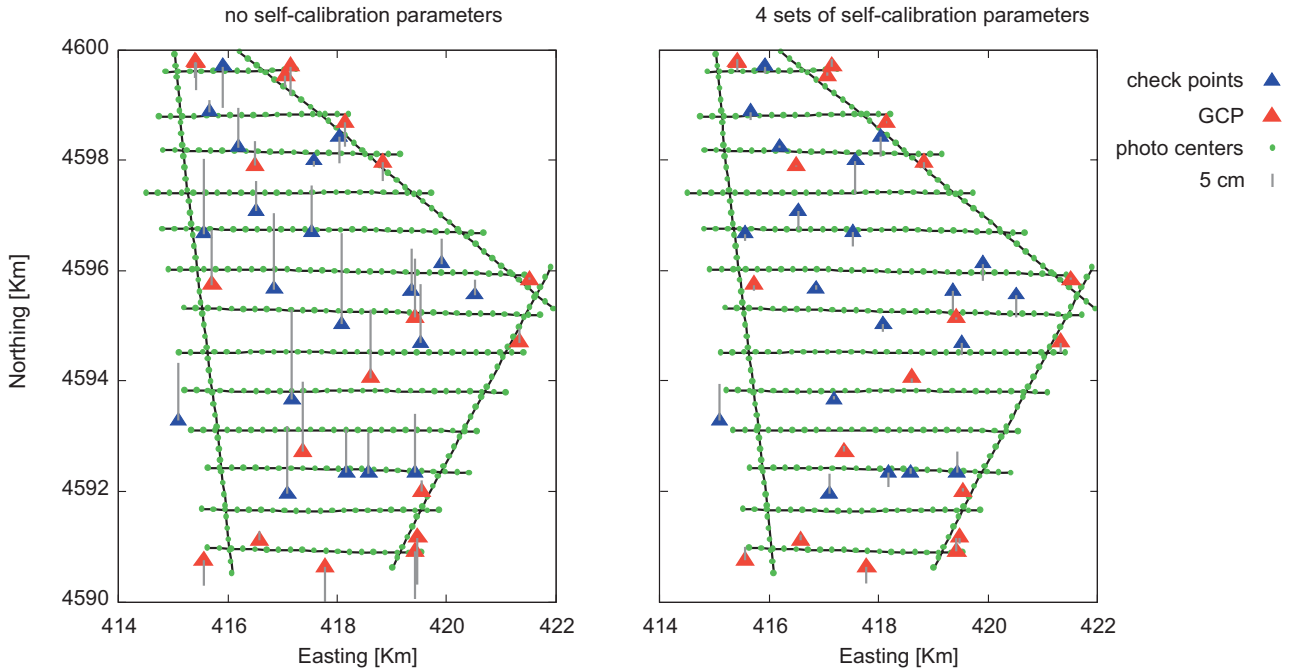

Figure 1: Rubí block point and height error distribution after triangulation. Left: no self-calibration parameters (similar to one single set - see table 3). Right: 4 sets of 12 self-calibration parameters.

The left part of figure 1 shows a systematic distribution of the height residuals with highly positive values in the block center and small or negative values at the borders. In order to evaluate a possible dependence of these height residuals on the block configuration, the Rubí block has been split into two sub-blocks: Rubí-N and Rubí-S. Rubí-N contains the 7 northernmost strips of the Rubí block and the overlapping parts of the transversal strips. Rubí-S contains the 7 southernmost strips of Rubí and the overlapping parts of the transversal strips. Rubí-N and Rubí-S have one strip, 4 GCP and some images of the transversal strips in common.

The three blocks Rubí, Rubí-N and Rubí-S were aerotriangulated without self-calibration and also with 4 sets of 12 self-calibration parameters leaving all other parameters unchanged. Figure 2 shows the height differences between the tie points resulting from aerotriangulation without self-calibration and with 4 sets of 12 self-calibration parameters.

On the left hand side of figure 2 the differences of the complete block is represented, the right hand side shows the differences of the two sub-blocks. The figure illustrates very well the systematic height error, which already is indicated in table 3 in case of no or 1 single set of self-calibration parameters and also by the height error distribution at the check points in figure 1. If no or only 1 set of self-calibration parameters is applied the point heights are systematically estimated too high. The height error depends on the location of the point and increases along with its distance from the border of the block. 4 sets of self-calibration parameters eliminate this systematic height shift as shown in table 3 and the right hand side of figure 2. This demonstrates clearly, that observed behavior does neither depend on aerial nor on ground control and that the existing DMC image geometry requires a self-calibration model, which properly takes into account the camera design involving 4 camera heads.

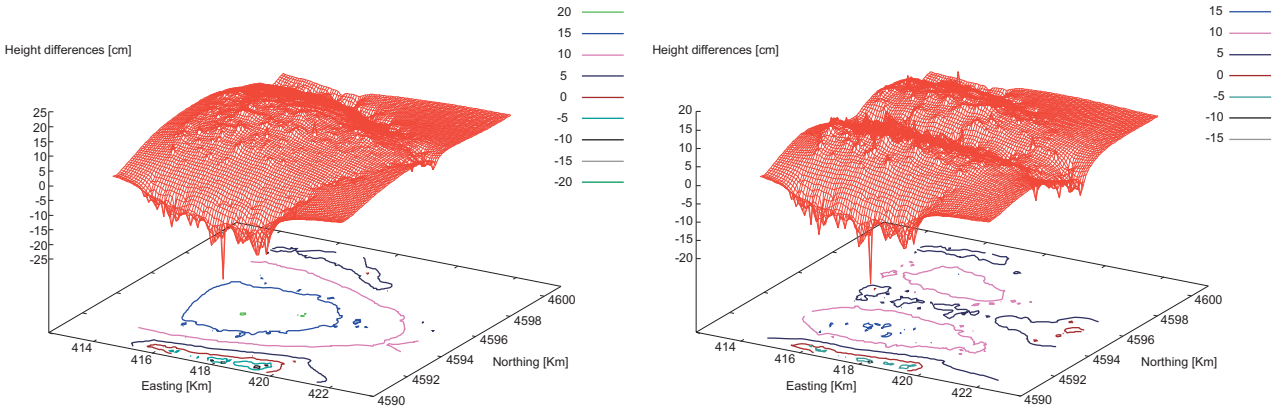

Figure 2: Height differences between tie points resulting from aerotriangulation without self-calibration and with 4 sets of 12 self-calibration parameters. Left: complete block Rubí. Right: block Rubí split into two sub-blocks.

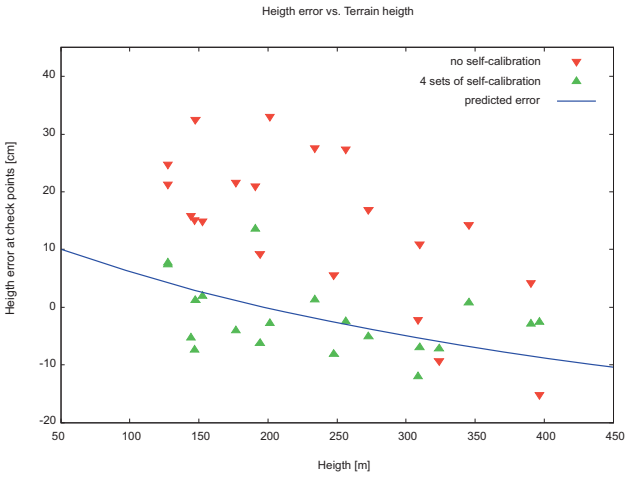

Figure 3: Height errors at check points plotted against point height. Red: errors without self-calibration. Green: errors using the 4 sets of 12 self-calibration parameters. Blue line: predicted height error according to Tang et al. (2000).

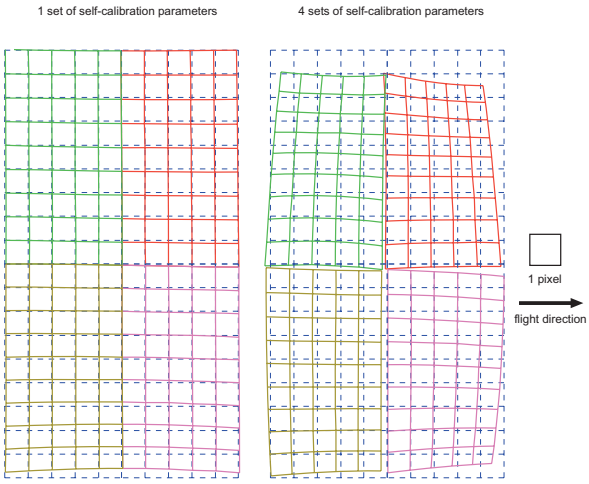

Figure 4: Image corrections produced by 1 set (left) and 4 sets of self-calibration parameters (right). The blue dashed grid represents the uncorrected DMC image. The corrected grids related to the 4 high-resolution camera heads are painted in different colors. The pixel size at the correction scale is represented on the right.

It is known, that the images of the 4 camera heads are fused to a DMC virtual image assuming a predefined mean terrain height for the block (Dörstel et al., 2003). It is also known, that a significant terrain height variation within the block, dependent on the flying altitude, introduces geometric errors to that fusion process, which are quantified in Tang et al. (2000). For the block Rubí (750 m flying altitude) a height deviation in the order of 100 m produces an error of 0.13 pixel in the image and a height error of 6.4 cm. In figure 3 the height error prediction is represented by the blue line. It is noticeable that results at check points using the 4 self-calibration sets of parameters match that error prediction fairly well. However, the results using no self-calibration parameters are worse than expected. In this case the predicted errors seem to be magnified by the un-modelled systematics of the camera.

Figure 4 shows the image corrections related to the estimated self-calibration parameters. A single parameter set (left sketch) yields no significant correction in image space. The 4 sets of parameters (right sketch) induce corrections of up to 1.5 pixels at the edges of the image. The four parameter sets and consequently the corrections in the four image quarters are significantly different indicating that each high resolution head might be affected by different systematic effects.

The full 4 sets of 12 parameters have also been estimated in the blocks Amposta, 415 and 419 flown on different dates and at different image scales. Figure 5 illustrates the respective corrections for each block. All of them show a clear trend in the image space, although the parameters are varying from block to block.

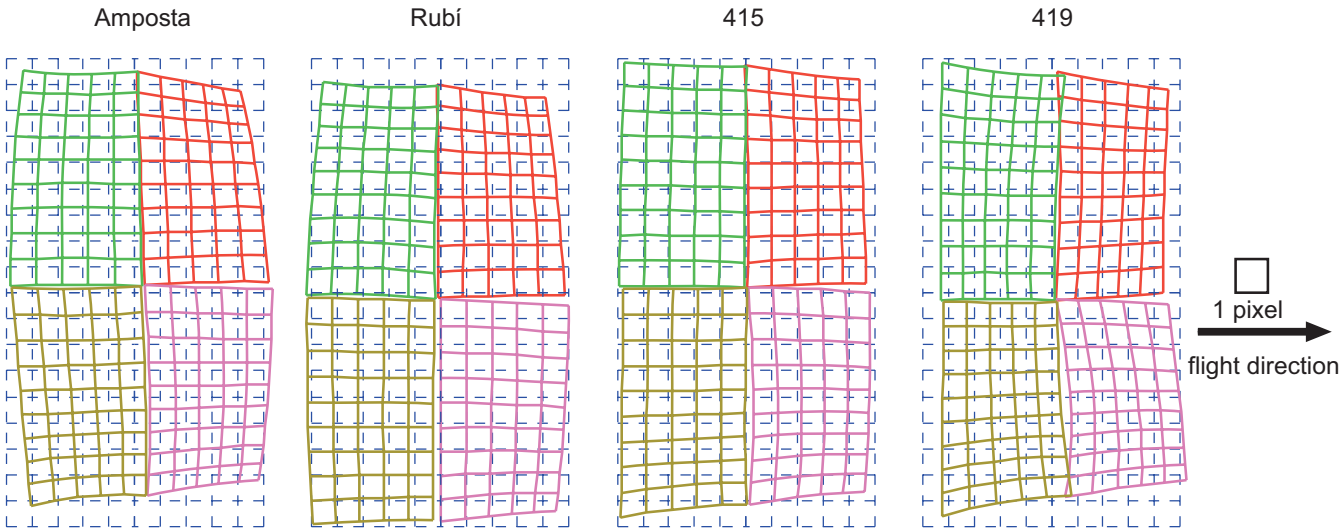

Figure 5: Image corrections produced by 4 sets of self-calibration parameters for the blocks Amposta, Rubí, 415 and 419

This section has shown that the commonly used 3+12 self-calibration parameter set is not capable to provide a significant accuracy improvement in aerotriangulation. Figure 5 also indicates that the image geometry might not be temporarily stable and/or depend on project parameters like image scale, terrain topography, etc. Further investigations at the ICC are planned to analyze these possible dependencies and also to substitute the used 12 parameter approach by a parameter set, which better represents the 4-camera head-geometry of the DMC in order to take the maximum benefit of this new technology.

3.3 Automatic DEM

In order to assess the quality of digital elevation models (DEM), in December 2004 the DMC was flown over half plain and half mountainous terrain with height differences of up to 1 000 m. The DMC images were taken with a GSD of 50 cm and 80% end lap. A larger block of the same area, flown in summer 2004 with a film RC30 camera at photo scale 1:30 000 and 80% end lap, served as a comparison. A more detailed description of these flight setups is given in Alamús et al. (2005).

A series of DEMs were automatically produced from the DMC as well as from the RC30 images using Intergraph's ISAE software (Krzystek, 1991), and the resulting grid point heights were compared with the ICC's DTM database. Its accuracy of 1.1 m (1σ) is actually too low to analyze all accuracy characteristics, especially in the flat area, but it is suitable for showing statistical trends, especially in the mountainous area. The results of this comparison are shown in table 4. Compared with the RC30 point heights, the DMC points are generally determined slightly better in the mountainous area and not so well in the flat area. The vertical shift between the DMC and the RC30 point heights of approximately 1 m might be caused by the different vegetation conditions in the different seasons of the year.

Camera	End lap	b/h	Mountainous area			Flat area		
			mean	rms	σ	mean	rms	σ
DMC	60 %	0.31	1.6	3.8	3.4	1.3	1.9	1.2
	80 %	0.15	1.7	3.8	3.3	0.9	1.5	1.3
RC30	60 %	0.58	0.5	3.7	3.6	0.1	0.8	0.8
	80 %	0.29	0.9	4.3	4.2	0.3	1.0	0.9

Table 4: Statistics of height differences [m] between automatically derived DEM grid points and ICC's DTM database

Due to the smaller DMC image format in flight direction, the b/h ratio only reaches approximately 50% of a conventional frame camera like the RC30, which consequently leads to 50% less height accuracy. According to the manufacturer of the DMC, this accuracy loss is compensated by the higher quality of the digital DMC image and consequently by a higher point measurement accuracy (Dörstel, 2003). We were able to confirm this fact in a series of automatic aerotriangulation runs, which resulted in a σ_0 of approx. 0.1 pixels, compared to approx. 0.3 pixels usually obtained with scanned conventional images. Although the geometrical result of a smaller b/h ratio is lower height accuracy, on the other hand the smaller difference in the viewing angles also improves point matching accuracy and reduces the probability of occlusions in mountainous areas. Therefore, the accuracy loss of the RC30 between 60% and 80% overlap is less than 50%. The low decrease of 12%-17% in this example might also be a consequence of the low-quality reference data. In the case of the DMC, the results for 60% and 80% end lap are more or less the same and in the flat terrain even 35% worse than the RC30, despite the superior DMC image quality. A possible explanation could be that the DMC results are influenced by a still unknown effect or even the lack of appropriate self-calibration (see 3.2), which produces a height error, which is bigger than the accuracy change caused by the b/h ratio.

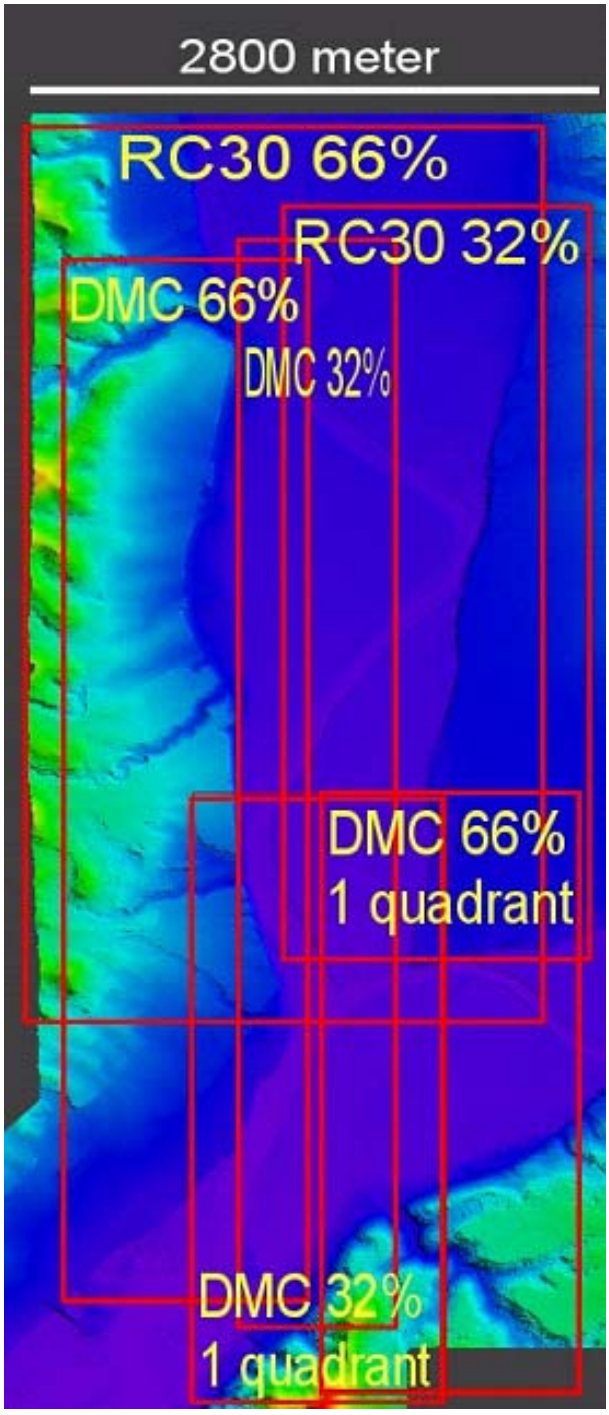

Figure 6: Location of the investigated models in the River Segre project.

In a new test setup we analyzed DMC images flown in June 2005 over the River Segre valley, where LIDAR data (1 point per m^2) was available for high-quality height reference with dm-accuracy, and also a larger block of the same area, flown in summer 2002 with a film RC30 camera at photo scale 1:22 000 and 60% end lap. A color coded representation of the LIDAR DEM and the location of the individual models investigated are depicted in figure 6. The DMC images were taken with a GSD of 50 cm and 60% end lap. They belong to a block of 312 photos, which was aerotriangulated three times: a) without self-calibration; b) with a global set of 12 self-calibration parameters; and c) using the extended model of self-calibration applying one set of 12 self-calibration parameters for each quadrant of the DMC image or each DMC camera head respectively, as described in section 3.2. For the accuracy analysis an automatic DEM for selected models was produced once again. Since ISAE generates DEM grid points close to the ground, the reference DEM was derived from ground classified LIDAR points at 2.5m grid space. The statistical results of the comparison between the DEM grid points and the LIDAR DEM are listed in table 5.

In the case of the RC30 the height accuracy change between 32% and 66% end lap is 35%. For the DMC data an accuracy change again is hardly visible and the extended model of 4x12 self-calibration parameters does not seem to affect the results at all. A possible explanation for this is that the ISAE software does not take into account any self-calibration, but calculates an absolute model orientation solely from the estimated ground points by resection. In order to properly analyze the influence of the different self-calibration models, a dense cloud point was generated in image space applying a region growing matching algorithm to just one quadrant of the DMC images, which later was rigorously transformed into object space using the estimated orientation (and self-calibration) parameters. Finally, all object points with y-parallaxes less than 0.2 pixels were compared to the LIDAR reference data and their height differences were statistically evaluated (see table 6).

In these results we can see a height accuracy improvement for the higher b/h ratio at 32% end lap, which is comparable to the improvement obtained with the RC30 camera in table 5. For 66% end lap the rigorously calculated points have more or less the same accuracy as the ISAE grid points, while a 32% end lap leads to 30% better accuracies. Comparing the different self-calibration versions a slight improvement in accuracy is visible if the extended 4x12 parameter model is applied. This also demonstrates an existing potential to improve the geometric modeling of the DMC camera and the processing of the virtual DMC images respectively. However, important questions still remain which could not been answered in this study, e.g. why a bigger b/h ratio is not reflected in an improved ISAE grid point accuracy and why the height accuracies derived from DMC images are always lower compared to the accuracies derived from RC30 images at the same b/h ratio and comparable image scale, despite the higher image pointing accuracy in DMC images (see table 1). In order to answer these questions new investigations are planned using more precise reference data collected in December 2005 during a simultaneous flight of the DMC, a RC30 and an Optech 3025 LIDAR system.

4. CONCLUSIONS

The initial evaluation tests (Alamús et al., 2005) showed that the point measurement accuracy in digital DMC images improves considerably while the 3D point accuracy remains more or less comparable to that of analog cameras. The results obtained are in agreement with the predicted DMC theoretical accuracies.

Camera	GSD	End lap	b/h	Self-calibration	Number of points	Min	Max	Mean	RMS	σ	σ_{norm}
RC30	0.33	66%	0.49	12 parameters	365 821	-12.40	14.48	0.17	0.53	0.50	0.68
		32%	0.98	12 parameters	182 754	-4.60	7.18	-0.08	0.38	0.37	0.50
DMC	0.45	66%	0.26	None	238 475	-26.66	25.55	0.43	1.13	1.04	1.04
				12 parameters	237 751	-31.68	27.07	0.47	1.09	0.98	0.98
				4 x 12 parameters	238 320	-27.52	24.38	0.42	1.12	1.04	1.04
		32%	0.52	None	156 339	-13.33	17.25	0.40	1.05	0.97	0.97
				12 parameters	157 356	-13.67	18.02	0.46	1.09	0.99	0.99
				4 x 12 parameters	145 209	-9.56	17.68	0.42	1.06	0.98	0.98

Table 5: Statistics of height differences [m] between automatically derived DEM grid points and the LIDAR reference DEM (last column contains standard deviation normalized to DMC GSD).

Camera	End lap	b/h	Self-calibration	Number of points	Min	Max	Mean	RMS	σ
DMC	66%	0.26	None	11171	-7.76	16.17	0.56	1.24	1.10
			12 parameters	10956	-7.90	16.22	0.59	1.24	1.09
			4 x 12 parameters	12597	-7.95	16.26	0.58	1.19	1.04
	32%	0.52	None	6625	-3.73	13.34	0.47	0.87	0.74
			12 parameters	6345	-3.66	13.36	0.50	0.90	0.74
			4 x 12 parameters	7331	-3.14	13.30	0.40	0.82	0.71

Table 6: Statistics of height differences [m] between rigorously calculated object points and the LIDAR reference DEM.

Significant self-calibration parameters have been obtained considering 4 independent sets of self-calibration parameters (one for each image quadrant) in the block adjustments. This approach is able to model the DMC systematic errors detected in the adjustments, allowing them to reach the theoretical accuracies and precision forecasted in the first published papers about DMC features, capabilities and accuracy. In particular, after applying these sets of parameters the height accuracy agrees with the theoretical analysis described in Tang et al. (2000). Further investigation should be done to understand the source of the systematic patterns and to derive more rigorous models to overcome them.

With respect to DEM accuracy, it would appear that DMC overcomes the handicap of the b/h ratio with its higher point accuracy in mountainous areas, but it is still barely noticeable in flat areas. Unfortunately, the data sets under study did not allow any final conclusion. Further work using data from a simultaneous flight with LIDAR, RC30 and DMC sensors will complete these studies on automatic DEM generation.

5. ACKNOWLEDGEMENTS

We gratefully thank the Institute of Photogrammetry and Geoinformation at the University of Hanover (Prof. C. Heipke) for leaving us the region growing matching software.

6. REFERENCES

Alamús R., Kornus W., Palà V., Pérez F., Arbiol R., Bonet R., Costa J., Hernández J., Marimon J., Ortiz M.A., Palma E., Pla M., Racero S., Talaya J., 2005. Validation process of the ICC digital Camera. In: ISPRS Hannover workshop 2005 “High-Resolution Earth Imaging for Geospatial Information”, 17-20th May 2005, Hannover (Germany).

Baron, A., Kornus, W., Talaya, J., 2003. ICC experiences on Inertial/GPS Sensor Orientation. In: ISPRS WG I/5 Workshop “Theory, Technology and Realities of Inertial/GPS sensor orientation”. 22-23rd September 2003, Castelldefels (Spain).

Colomina, I., Navarro, J., Termens, A., 1992. GeoTeX: A general point determination system. In: Proceedings of the IntArchPhRs, Com. II, Vol XXIX, pp 656-664.

Dörstel, C., 2003. DMC- Practical Experiences and Photogrammetric System Performance. In: Photogrammetric Week 2003 Fritsh D. (Ed.), September 2003 Sttutgart (Germany), pp. 59-65.

Dörstel, C., Jacobsen, K., Stallmann, D., 2003. DMC - Photogrammetric Accuracy – Calibration aspects and generation of synthetic DMC images. In: Grün A., Kahmen H.(Eds.) Optical 3-D Measurement Technics VI, Vol. I, Intitut fot Geodesy and Photogrammetry, ETH, Zürich, pp 74-88.

Ebner, H., 1976. Self-calibrating block adjustment. In: Congress of the International Society for Photogrammetry. Invited paper of Commission III, 1976, Helsinki (Finland).

Hinz A., 1999. The Z/I Digital Aerial Camera System. In: Proceedings of the 47th Photogrammetric Week. 1999, Stuttgart (Germany), pp. 109-115.

Krzystek P., 1991. Fully Automatic Measurement of Digital Elevation Models. In: Proceedings of the 43th Photogrammetric Week. 1991, Stuttgart (Germany), pp. 203-214.

Tang, L., Dörstel, C., Jacobsen, K., Heipke, C., Hinz, A.: Geometric Accuracy Potential of the Digital Modular Camera. Proceedings of the ISPRS Congress, Vol. XXXIII, Vol. I/3, Amsterdam, 2000.

Zeitler, W., Dörstel, C., Jacobsen, K., 2002. Geometric Calibration of the DMC: Method and Results. In: IntArchPhRs, Com. I, Denver (USA), Vol XXXIV Part 3b, pp 324-333.